Greatly Enhanced Magneto-optic Detection of Single Nanomagnets Using Focused Magnetoelastic Excitation

Wei-Gang Yang* and Holger Schmidt

School of Engineering, University of California Santa Cruz, 1156 High Street, Santa Cruz, California 95064, USA

ABSTRACT

Magnetization dynamics of nanomagnets directly determine the performance of magnetic storage and memory devices. Here, we report a 10-times enhancement of magnetization dynamics excitation of single nanomagnets using focused surface acoustic waves (SAWs), compared to conventional optical excitation. SAWs are generated via ultrafast optical excitation of an arc-shaped phononic grating and focused onto a single nanomagnet located at the focal spot of the grating. Thanks to the robust resonance excitation, we observe the strain-controlled ultrafast magnetization dynamics in a sub-100 nm single nanomagnet. This improved excitation efficiency was applied to exciting SAWs in four sets of gratings with different pitches using a single laser spot. This enabled selective excitation of any one of four identical nanomagnets at different frequencies simply via tuning an external magnetic field. This all-optical technique provides a method of addressing individual magnetic nano-oscillators and study their intrinsic magnetization dynamics.

* To whom correspondence should be addressed: wyang27@ucsc.edu

Nanomagnets have been identified as leading candidates for next generation data storage, quantum computation, low power magnetic logic and neuromorphic computing. [1–3] The operation characteristics of these technologies depend critically on dynamic magnetic properties of the nanomagnets. Thus, the direct measurement of magnetization dynamics in a single nanomagnet is important for the development of nanostructured magnetic devices. There are only a few approaches such as time-resolved magneto-optic Kerr effect (TRMOKE) [4], spin-torque ferromagnetic resonance (ST-FMR) [5,6], time-resolved magnetic X-ray microscopy [7], photoemission electron microscopy (PEEM) [8,9] and heterodyne magneto-optical microwave microscopy (H-MOMM) [10] that have shown this capability.

Recently, we introduced an all-optical technique to excite and probe the magnetization dynamics of a single nanomagnet via magnetoelastic (MEL) coupling. [11] Surface acoustic waves (SAWs) were optically generated by a one-dimensional nanowire array [11,12] and used to excite narrow-band magnetization precessions in a single nanomagnet without heating it. [11] For optical detection, the diffraction-limited probe beam size is much larger than the nanomagnet, adversely affecting the signal-to-noise ratio (SNR). [13] The all-optical method produces a larger magnetization excitation, which offers a solution of measuring single nanomagnets smaller than 200 nm.

Focusing the mechanical energy of the SAW at the location of the nanomagnet greatly improves the method. Previously, focused SAWs with wavelengths (λ) of ~10 μm were used to sort single particles, cells and droplets. [14] Focused SAWs (λ = ~20 μm) were also used to assist magnetization switching in a ~3 μm large region of a FeGa thin film because the SAW lowers the coercivity field at the focal point. [15] In this work, we observe a greatly enhanced magneto-optic response by focusing SAWs onto a remote single nanomagnet. Here, we employ SAWs with almost two orders of magnitude shorter wavelengths (~400 nm) to focus the acoustic energy more efficiently down to a ~100 nm spot. [15] The magneto-optic signal amplitude of the focused SAW (FSAW) driven magnetization dynamics is almost an order of magnitude larger than that of optically (i.e. heat pulse) triggered magnetization dynamics, i.e. using all-optical TRMOKE technique when comparable pump fluences are used. We report elastic strain-controlled magnetization dynamics in a sub-100 nm single nanomagnet. This ability has important implications for strain-assisted switching [15–17] that has recently attracted significant attention due to its potential applications including magnetic memory and logic, and non-Boolean circuits. [18,19] Very recently, spin waves with large amplitude and long travelling distance have been successfully generated in a Ni thin film by SAWs [20], which might be further improved by using the Focused SAW technique. Finally, we show the capability of selectively activating any one of four identical nanomagnets at different frequencies via an integrated phononic grating design that includes four different pitches of arc-shaped bars. When a pump beam illuminates the integrated grating, four different wavelength SAWs simultaneously launch and separately excite the magnetization dynamics of the

single nanomagnets at different frequencies ranging from 7 GHz to 10 GHz at corresponding resonant fields. This ability has implications for nanosized oscillators [21] due to the tunable operating frequency in the gigahertz range, which shows potential for wireless and radar communication. [22]

For the optical excitation measurements, isolated nickel (Ni) nanomagnets (30 nm thick) with diameters (D) ranging from 75 nm to 200 nm were fabricated without surrounding gratings (**Fig. 1a**) by utilizing electron beam lithography (EBL), electron beam evaporation, and lift-off processes.[11] Before the nanomagnet fabrication, Si substrate was capped by a 110 nm thick hafnium oxide antireflection (AR) coating. [13,23] In order to investigate SAW and FSAW driven magnetization excitation of single nanomagnets, the same batch of single Ni nanomagnets were defined between two sets of straight (**Fig. 1b**) (Pitch = ~400 nm) and arc-shaped Ni gratings (**Fig. 1c**) (Pitch ~400 nm, focal distance ~2 μm and arc angle 120°). The magnetization dynamics were analyzed using the TRMOKE technique. [24] The pump pulse was generated by second harmonic generation of an ultrafast Ti:Sapphire laser and then then focused onto the sample surface using a microscope objective (M = 100X, N.A. = 0.9, λ = 400 nm, pulse width = 150 fs, FWHM = ~4.5 μm). A mechanically delayed probe pulse (λ = 800 nm, pulse width = 150 fs, FWHM = 0.58 μm) was focused onto the nanomagnet and experienced a gyrotropic polarization rotation upon reflection. For the conventional optical excitation measurements, the center of pump overlapped with that of the nanomagnet (**Fig. 1d**), while for the SAW and FSAW excitation, the center of pump was at least 4.5 μm away from the nanomagnet to ensure there was negligible photoexcitation of the spin system (**Figs. 1e, 1f**). Knife-edge measurements were performed on both the pump and probe beams to determine their exact spatial character. The frequency of the SAW (f_{SAW}) was determined by the ratio between the speed of sound in the HfO_2 (v_{sound} ~ 3 km/s) and the pitch (p) of the Ni bars via the relation $f_{SAW}=v_{sound}/p$. The Ni nanomagnets were ~2 μm away from the grating (**Figs. 1b, 1c**) so that the probe (FWHM = 0.58 μm) only detected the magnetic signal of the Ni nanomagnet. Lock-in detection at the pump modulation frequency was used to record the Kerr rotation (magnetic) as well as the elastic motion (nonmagnetic) using the difference and sum signal of a balanced photodetector setup, respectively.[25] A variable external applied field (H_{app}) with an in-plane component parallel to the propagation direction of the SAWs was held at a fixed angle θ_H = 30° from the surface normal. The field was provided by two permanent magnets under the sample. A program-controlled motor moved the magnets to a specific position corresponding a field angle and magnitude.

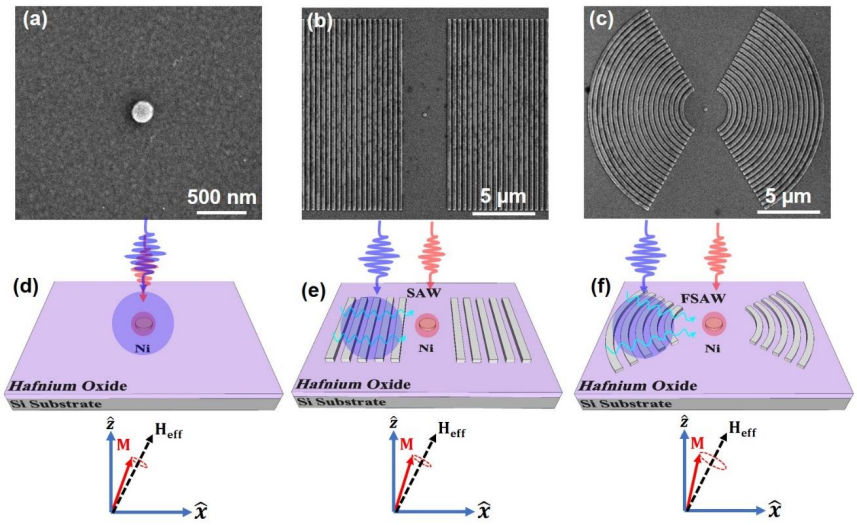

FIG. 1. SEM images of (a) an isolated Ni nanomagnet without surrounding gratings, Ni nanomagnets surrounded by (b) straight and (c) arc-shaped gratings (pitch = 400 nm). Schematic plots of (d) optical, (e) SAW-driven and (f) FSAW-driven magnetization excitation in single Ni nanomagnets. The red and blue regions represent relative positions between the probe and pump beams, respectively. The illustrations below (d), (e) and (f) indicate magnetic precession with different amplitude around the effective field for these three different configurations at the applied field of ~2.6 kOe, respectively.

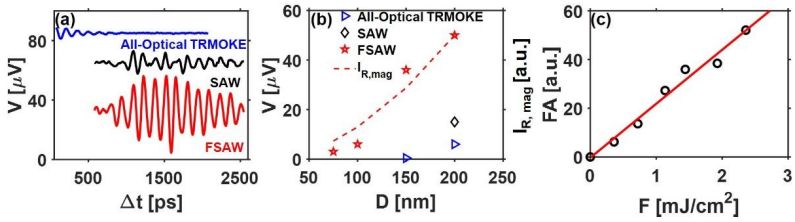

FIG. 2. (a) Time traces of the optically excited 200 nm Ni single nanomagnet, i.e. via All-Optical TRMOKE, the SAW and FSAW driven identical single nanomagnets. (b) Magneto-optical signal amplitude of single nanomagnets measured by three different configurations and the calculated relative intensity of the light reflected from the nanomagnets ($I_{R,mag}$). (c) The Fourier amplitude (FA) of the FSAW-driven magnetization dynamics at ~7 GHz as a function of the pump fluence (F) on the arc-shaped gratings, and the red line is a linear fit to the data.

In terms of the excitation mechanisms, for the All-Optical TRMOKE technique (**Fig. 1d**), the pump quasi-instantaneously demagnetizes the nanomagnet [26], and within picoseconds the magnetization is restored and

subsequently follows a helical trajectory back to the equilibrium orientation, while for the SAW or FSAW excitation (**Figs. 1e,f**), the acoustic pulses periodically deform the nanomagnet in time and space, which in turn generates an internal MEL field (H_{MEL}) [27] that triggers spin dynamics in single nanomagnets at the acoustic frequency. **Fig. 2a** shows a stark comparison of three nominally identical single nanomagnets excited by heat pulses (All-Optical TRMOKE), optically generated SAWs and FSAWs, respectively. First, it is worth noting that the magnetic oscillation response driven by the SAW and the FSAW is delayed compared to the one caused by the thermal pulses because it takes time for the strain waves to travel from the illuminated gratings to the nanomagnet. The FSAW-driven magnetic oscillation is increased by a factor of 3-4 compared to the SAW-driven one. We compare the lock-in voltage signal of SAW and FSAW from the TRMOKE non-magnetic channel and observe that the amplitude signal of FSAW is ~ 3.3 times larger than that of the SAW around the time delay of 1.5 ns when the maximum magnetoelastic excitation occurs. Therefore, the increase in magnetic oscillation is in excellent agreement with the increase in SAW amplitude. The increase might be further improved by optimizing arc degree, geometric focal length and FSAW wavelength. [28]. The enhancement of the magnetization excitation as a result of the increase in SAW amplitude can be understood by considering the MEL energy density (U_{MEL}) and H_{MEL} using the following relationships [27]:

$$U_{MEL} = \frac{B_1}{M_S^2}\sum_i M_i^2\,\varepsilon_{ii} + \frac{B_2}{M_S^2}\sum_i\sum_{j\neq i} M_i\,M_j\,\varepsilon_{ij} \quad (1)$$

$$H_{MEL} = -\frac{\delta U_{MEL}}{\delta \vec{M}} \quad (2)$$

where B_1 and B_2 are the magnetoelastic constants ($7.85\text{x}10^7$ erg/cm for Ni) and ε is the 3-dimensional strain tensor. Thus, H_{MEL} is significantly increased due to the increased elastic strain by focusing the SAW to the nanomagnet per equations (1) and (2). The larger time-varying H_{MEL} acts a driving term in the total effective field and thus initiates larger precession when the intrinsic magnetic response approaches resonance with the time-varying H_{MEL}. Second, we observe that the dynamic Kerr signal amplitude of the single nanomagnet due to the FSAW driven magnetization dynamics is almost 10 times larger than that measured by the All-Optical TRMOKE technique. Due to the almost identical total intensity of the reflected probe beam from these identical single nanomagnets, the dramatic enhancement of the magneto-optic signal amplitude can only be attributed to the FSAW-triggered greatly enhanced magnetic precession amplitude, indicating highly efficient MEL coupling and narrow-band excitation. Consequently, the spatial sensitivity of the magneto-optic detection is also significantly improved as shown in **Fig. 2b**. For the optical excitation, it is challenging to detect single nanomagnets smaller than 200 nm in diameter, while we are able to excite and probe the magnetization dynamics of the nanomagnet diameter as small as 75 nm by using the FSAW, which is smaller than those in previous reports using magnetoelastic excitation method. [29,30] Here, we

calculate the intensity of the light reflected from the single nanomagnets ($I_{R,mag}$) based on a geometric model [10]: $I_{R,mag} = R_{mag} \int_0^{D/2} 2\pi r I_0(r)\, dr$, where R_{mag} is the reflection coefficient and $I_0(r) \propto e^{-2r^2/\omega_0^2}$. The variation of $I_{R,mag}$ (red dashed line) is in excellent agreement with that of magneto-optical signal detected from the nanomagnets using FSAW excitation. We also study the dependence of FSAW-driven magnetization dynamics on the pump fluence. We took the FSAW-driven TRMOKE scans at a series of pump fluences and Fourier-transformed the TRMOKE data to the frequency domain. **Fig. 2c** shows an almost linear increase of the Fourier amplitude with increasing pump fluence because the amplitude of SAWs scales linearly with the pump power [31], which suggests that the magnetic precession amplitude can be modulated by the strength of the optically generated elastic strain.

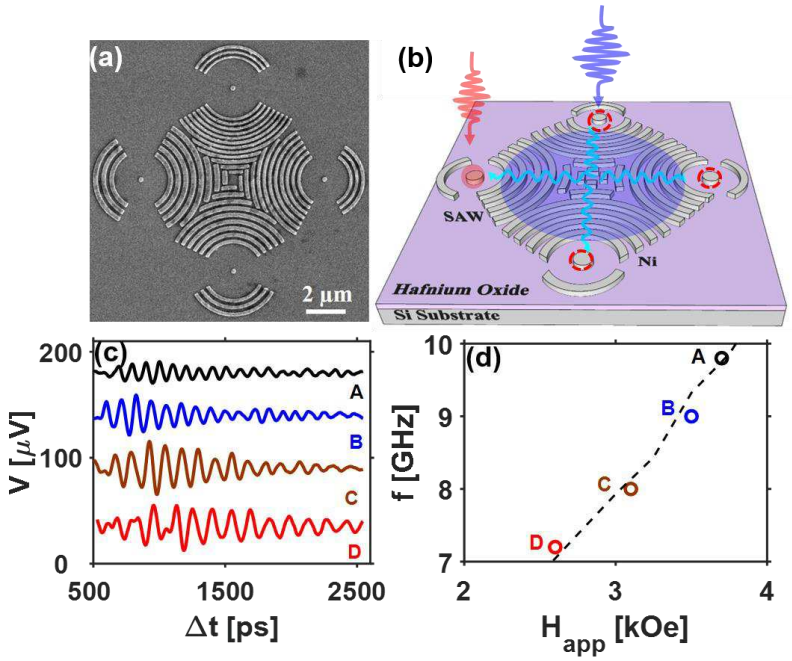

FIG. 3. (a) SEM image of four identical Ni nanomagnets (A, B, C and D) surrounded by corresponding four different pitches of gratings with pitch = 250 nm, 300 nm, 350 nm, 400 nm, respectively. (b) Schematic plot of FSAW-driven magnetization excitation in four identical Ni nanomagnets. (c) Time traces of the FSAW-driven four nanomagnets. (d) The precession frequency of the four nanomagnets at corresponding resonant fields. The dashed line is the magnetic frequencies of a single nanomagnet measured using all-optical TRMOKE.

With this improved excitation efficiency, we can now use a single optical pump pulse to excite multiple distinct SAWs that selectively drive spatially separated individual nanomagnets. In order to demonstrate this capability, we integrate four different sets of gratings with different pitches, as shown in **Fig. 3a**. When the pump pulses are focused at the center of the structure, four SAWs with different frequencies are simultaneously launched and focused onto the four identical nanomagnets labeled as "A", "B", "C", "D", respectively. The probe beam (**Fig. 3b**) is used to successively probe the FSAW-driven magnetization dynamics in the four nanomagnets at the corresponding four different resonant fields. **Fig. 3c** shows the FSAW-driven magnetization dynamic response of the four nanomagnets at the corresponding resonant fields (H_{app} = 3.7 kOe, 3.5 kOe, 3.1 kOe and 2.6 kOe, respectively). The integrated gratings enable us to drive individual nanomagnets at different frequencies using magneto-elastic control. Moreover, the FSAW excitation can excite only a single mode due to its narrow-band resonant excitation characteristics. Figure 3d summarizes the FSAW-driven precession frequency (f) and corresponding resonant fields of these four nanomagnets, which shows that we are able to selectively activate microwave oscillations in any one nanomagnet at different frequencies by simply altering the external magnetic field

In conclusion, we observe a dramatic enhancement of the magnetoelastic excitation of a single nanomagnet by focusing surface acoustic waves onto the nanomagnet compared to the conventional TRMOKE technique using the optical excitation. We report the magnetoelastically controlled magnetization dynamics in a sub-100 nm single nanomagnet. Moreover, one might be able to improve further the magneto-optical detection spatial sensitivity by using materials with stronger magnetoelastic effects such as CoFeB and FeGaB and optimizing the phononic grating design. Therefore, the technique may open an avenue of studying small nanoscale magnets using all-optical methods. Finally, using multiple phononic gratings, we present the selective activation of magnetization dynamics of single nanomagnets, via varying an external field, which has implications for SAW-driven nano-oscillators.

We acknowledge fruitful discussions with M. Jaris and T. Yuzvinsky, and support by the W.M. Keck Center for Nanoscale Optofluidics at UC Santa Cruz. This work was supported by the National Science Foundation under Grants No. ECCS-1509020 and DMR-1506104.

REFERENCES

[1] B. Behin-Aein, D. Datta, S. Salahuddin, and S. Datta, Nat. Nanotechnol. **5**, 266 (2010).

[2] J. Torrejon, M. Riou, F.A. Araujo, S. Tsunegi, G. Khalsa, D. Querlioz, P. Bortolotti, V. Cros, K. Yakushiji, A. Fukushima, H. Kubota, S. Yuasa, M.D. Stiles, and J. Grollier, Nature **547**, 428 (2017).

[3] D. Bhowmik, L. You, and S. Salahuddin, Nat. Nanotechnol. **9**, 59 (2014).

[4] A. Barman, S. Wang, J.D. Maas, A.R. Hawkins, S. Kwon, A. Liddle, J. Bokor, and H. Schmidt, Nano Lett. **6**, 2939 (2006).

[5] C. Wang, Y.T. Cui, J.A. Katine, R.A. Buhrman, and D.C. Ralph, Nat. Phys. **7**, 496 (2011).

[6] M.B. Jungfleisch, J. Ding, W. Zhang, W. Jiang, J.E. Pearson, V. Novosad, and A. Hoffmann, Nano Lett. **17**, 8 (2017).

[7] S. Bonetti, R. Kukreja, Z. Chen, F. Macià, J.M. Hernàndez, A. Eklund, D. Backes, J. Frisch, J. Katine, G. Malm, S. Urazhdin, A.D. Kent, J. Stöhr, H. Ohldag, and H.A. Dürr, Nat. Commun. **6**, 8889 (2015).

[8] M. Foerster, F. Macià, N. Statuto, S. Finizio, A. Hernández-Mínguez, S. Lendínez, P. V. Santos, J. Fontcuberta, J.M. Hernàndez, M. Kläui, and L. Aballe, Nat. Commun. **8**, 407 (2017).

[9] X. Wang, D.J. Keavney, M. Asmat-Uceda, K.S. Buchanan, A. Melikyan, and X.M. Cheng, Appl. Phys. Lett. **105**, 102408 (2014).

[10] H.T. Nembach, J.M. Shaw, C.T. Boone, and T.J. Silva, Phys. Rev. Lett. **110**, 117201 (2013).

[11] W.G. Yang, M. Jaris, D.L. Hibbard-Lubow, C. Berk, and H. Schmidt, Phys. Rev. B **97**, 224410 (2018).

[12] C.L. Chang, R.R. Tamming, T.J. Broomhall, J. Janusonis, P.W. Fry, R.I. Tobey, and T.J. Hayward, Phys. Rev. Appl. **10**, 034068 (2018).

[13] N. Qureshi, S. Wang, M.A. Lowther, A.R. Hawkins, S. Kwon, A. Liddle, J. Bokor, and H. Schmidt, Nano Lett. **5**, 1413 (2005).

[14] D.J. Collins, A. Neild, and Y. Ai, Lab Chip **16**, 471 (2016).

[15] W. Li, B. Buford, A. Jander, and P. Dhagat, J. Appl. Phys. **115**, 17E307 (2014).

[16] I.S. Camara, J.Y. Duquesne, A. Lemaître, C. Gourdon, and L. Thevenard, Phys. Rev. Appl. **11**, 014045 (2019).

[17] A. Roe, D. Bhattacharya, and J. Atulasimha, Appl. Phys. Lett. **115**, 112405 (2019).

[18] V. Sampath, N. D'Souza, D. Bhattacharya, G.M. Atkinson, S. Bandyopadhyay, and J. Atulasimha, Nano Lett. **16**, 5681 (2016).

[19] N. D'Souza, M. Salehi Fashami, S. Bandyopadhyay, and J. Atulasimha, Nano Lett. **16**, 1069 (2016).

[20] B. Casals, N. Statuto, M. Foerster, A. Hernández-Mínguez, R. Cichelero, P. Manshausen, A. Mandziak, L. Aballe, J.M. Hernàndez, and F. Macià, Phys. Rev. Lett. **124**, 137202 (2020).

[21] S.I. Klselev, J.C. Sankey, I.N. Krivorotov, N.C. Emley, R.J. Schoelkopf, R.A. Buhrman, and D.C. Ralph, Nature **425**, 380 (2003).

[22] D. Li, Y. Zhou, B. Hu, J. Åkerman, and C. Zhou, Phys. Rev. B **86**, 014418 (2012).

[23] S. Wang, A. Barman, H. Schmidt, J.D. Maas, A.R. Hawkins, S. Kwon, B. Harteneck, S. Cabrini, and J. Bokor, Appl. Phys. Lett. **90**, 252504 (2007).

[24] C. Berk, M. Jaris, W. Yang, S. Dhuey, S. Cabrini, and H. Schmidt, Nat. Commun. **10**, 2652 (2019).

[25] Y. Yahagi, C.R. Berk, B.D. Harteneck, S.D. Cabrini, and H. Schmidt, Appl. Phys. Lett. **104**, 162406 (2014).

[26] E. Beaurepaire, J.C. Merle, A. Daunois, and J.Y. Bigot, Phys. Rev. Lett. **76**, 4250 (1996).

[27] Y. Yahagi, B. Harteneck, S. Cabrini, and H. Schmidt, Phys. Rev. B **90**, 140405(R) (2014).

[28] S.K.R.S. Sankaranarayanan and V.R. Bhethanabotla, J. Appl. Phys. **103**, 064518 (2008).

[29] S. Mondal, M.A. Abeed, K. Dutta, A. De, S. Sahoo, A. Barman, and S. Bandyopadhyay, ACS Appl. Mater. Interfaces **10**, 43970 (2018).

[30] W.G. Yang, M. Jaris, C. Berk, and H. Schmidt, Phys. Rev. B **99**, 104434 (2019).

[31] D. Li and D.G. Cahill, Phys. Rev. B **94**, 104306 (2016).